Modeling and Simulation of High Blocking Voltage in 4H Silicon Carbide Bipolar Junction Transistors

Hamid Fardi[1*]

[1]*Department of Electrical Engineering, University of Colorado Denver, United States of America.*

ABSTRACT

For a given breakdown voltage, the drift region thickness and doping concentration of punch-through structure can be optimized to give the lowest specific on-resistance. An optimization scheme performed for a breakdown voltage of 14 kV in 4H-SiC bipolar junction transistor (BJT) at 300 K. The optimum drift region thickness and doping concentration for a 4H-SiC punch-through structure at different breakdown voltages are presented. The optimum drift region thickness and doping concentration are 114 *μm* and $6.6\times10^{14}cm^{-3}$, respectively, which results in the lowest specific on-resistance of 117 mΩcm². The specific on-resistance is compared with the theoretical specific on-resistance of non punch-through structure. It is shown that the optimized punch-through structure not only has a thinner drift region, but also has a slightly lower specific on-resistance than non punch-through structure. The model is applied and compared to a measured 4H-SiC bipolar transistors with high blocking voltage and results are discussed. The experimental 4H-SiC BJT is able to block 1631 V at 300 K and 2033 V at 523 K, respectively and when the base is open. The simulated blocking voltage when base is open is slightly lower (1600 V at 300 K) than the experimental value due to the current-amplifying properties of the common-emitter BJT.

Keywords: Device Modeling, Silicon Carbide, Bipolar Junction Transistors

1. Introduction

Although many improvements have been made in silicon material technology and in the design of new device structures, the silicon-based power devices are rapidly approaching their theoretical limits of performance [1,2]. As shown in Table 1, when compared to silicon, 4H-SiC offers a lower intrinsic carrier concentration (9 to 37 orders of magnitude), a higher electric breakdown field (4 to 18 times), a higher thermal conductivity, and a larger saturation electron drift velocity 2 to 2.7 times higher [3-6]. Because of high electric breakdown field, the drift region can be much thinner than that of their Si

E-mail address: hamid.fardi@ucdenver.edu.

counterparts for the same voltage rating, thus a much lower specific on-resistance could be obtained. With lower specific on-resistance, wide-bandgap-based power devices have lower conduction losses and higher overall efficiency. Because of high-saturation drift velocity power devices based on wide-bandgap materials could be switched at higher frequencies than their Si counterparts. Moreover, the charge in the depletion region of a PN junction can be removed faster if the drift velocity is higher, and therefore, the reverse recovery time is shorter.

Table 1. Physical parameters and bias variables

Physical Parameters and Variables	Unit	Value
Electron mobility, μ_n	cm^2/V-s	347
Hole mobility, μ_p	cm^2/V-s	34.5
Electron lifetime, τ_n	ns	22
Hole lifetime, τ_p	ns	5.7
Collector series resistance, R_C	Ω	1.24
Collector-Emitter Bias, V_{CE}	V	-
Collector Current, I_C	A	-
Base Current, I_B	A	-

Breakdown electric field in 4H-SiC is almost one order of magnitude higher than silicon, which makes 4H-SiC superior in high voltage applications. The high breakdown electric field in 4H-SiC allows power devices to use a much thinner and to use higher-doped drift layer, hence significantly reduces the specific on-state [7, 8].

The fabrication and characterization of a 4H SiC bipolar junction transistor with double base epilyer is to improve specific on-resistance [9, 10]. A lateral BJT structure with surface electric field optimization technique is shown to achieve a high breakdown voltage and lower specific on resistance reported in several articles including [11-16]. Due to the advantages of 4H-SiC devices such as low specific on-resistance, high thermal stability, and high blocking voltage, SiC MOSFET and BJTs are considered a better alternative to Si IGBTs [17- 24]. Recently 4H-SiC bipolar junction transistors with a blocking voltage in the range of 0.75 kV to 9.2 kV and with an on-state resistance of 2.9 mΩcm^2 to 49 mΩcm^2 are reported [25-27].

In this study, a two-dimensional numerical analysis tool ATLAS [11] is used to investigate the electrical characteristics in 4H-SiC bipolar transistors. The simulation and theoretical model are compared to the measured 4H-SiC bipolar junction transistors. An optimization model is presented to obtain the lowest specific on-resistance. It is shown that a punch-through structure not only has a thinner drift region, but also can have a slightly lower specific on-resistance than a non punch-through structure. It is also shown that the simulated blocking voltage is slightly lower when base is open due to the current-amplifying properties of the common-emitter bipolar junction transistors.

2. Modeling Ionization Coefficients

In high electric field, free carriers can obtain enough energy to cause impact ionization. This process can be understood as the inverse process to the Auger recombination. The reciprocal of the carrier mean free path is called the impact ionization coefficient. With these coefficients of electrons and holes, the generation rate *G* due to impact ionization can be expressed as

$$G = \alpha_n n v_n + \alpha_p n v_p \tag{1}$$

where α_n and α_p denote the impact ionization coefficients of electrons and holes, v_n and v_p are the electron and hole drift velocities, receptively. α_n and α_p are modeled with Chynoweth equation [28]:

$$\alpha(E) = \gamma\alpha_0 \exp\left(-\frac{\gamma b}{E}\right) \tag{2}$$

where *E* is the electric field and α_0 and *b* are fitting parameters:

$$\gamma(T) = \frac{\tanh\left(\frac{h\omega_{op}}{2kT_0}\right)}{\tanh\left(\frac{h\omega_{op}}{2kT}\right)} \tag{3}$$

The parameter γ and the optical phonon energy $h\omega_{op}$ relate the temperature dependence of phonon gas against the accelerated carriers. Both $\gamma\alpha_0$ and γb depend on lattice temperature (*T*). However, the term γb is shown experimentally to be independent of the temperature in SiC [29]. Therefore, the empirical model suggested by Okuto and Crowell is used in the simulation [30]:

$$\alpha(E) = a\cdot\left[1 + c\cdot(T - 300K)\right]\cdot E^{\gamma_1}\cdot\exp-\left[\frac{b\cdot\left(1 + d\cdot(T - 300K)\right)}{E}\right]^{\gamma_2} \tag{4}$$

where *a*, *b*, *c*, *d*, γ_1 and γ_2 are fitting parameters [14]. By fitting the experimental results in with Eq. (4), the impact ionization coefficients α_n and α_p are expressed as below [31]:

$$\alpha_n(E,T) = 7.26\times10^6\left(1 - 1.47\times10^{-3}(T - 300K)\right)\exp\left(-\frac{2.34\times10^7}{E}\right)cm^{-1} \tag{5}$$

$$\alpha_p(E,T) = 6.85\times10^6\left(1 - 1.56\times10^{-3}(T - 300K)\right)\exp\left(-\frac{1.41\times10^7}{E}\right)cm^{-1} \tag{6}$$

2.1 Critical Field of 4H-SiC Power Transistors

For power devices, the high blocking voltage is usually supported by a thick lightly doped drift layer. Since the drift layer is thick and low-doped, its resistance may dominate the on-resistance of the power device. The critical field in 4H-SiC is dependent on the doping and the avalanche breakdown due to impact ionization will occur when the electric field exceeds the critical field (E_{cr}) modeled by the following equation:

$$E_{cr} = \frac{2.49\times10^{6}}{1-\frac{1}{4}\log_{10}\left(\frac{N}{10^{16}cm^{-3}}\right)} V/cm \tag{7}$$

where N is the doping concentration.

2.2 Drift Layer Design for Non-Punch-Through Structure

The theoretical specific on-resistance R_{SP_ON} associated with the drift layer is

$$R_{SP\_ON} = resistance \cdot area = \frac{W}{q\mu_n N_D} = \frac{4V_{BR}^2}{\varepsilon_s \mu_n E_{cr}^3} \tag{8}$$

where V_{BR} is the breakdown voltage, ND is the drift layer doping concentration and ε_s is the dielectric constant of the semiconductor, and μ_n and W are the drift layer electron mobility and thickness, respectively. The above equation shows that the specific on-resistance of 4H-SiC drift layer can be about 550 times lower than that of silicon drift layer for the same voltage rating due to the higher critical field in 4H-SiC junction transistors.

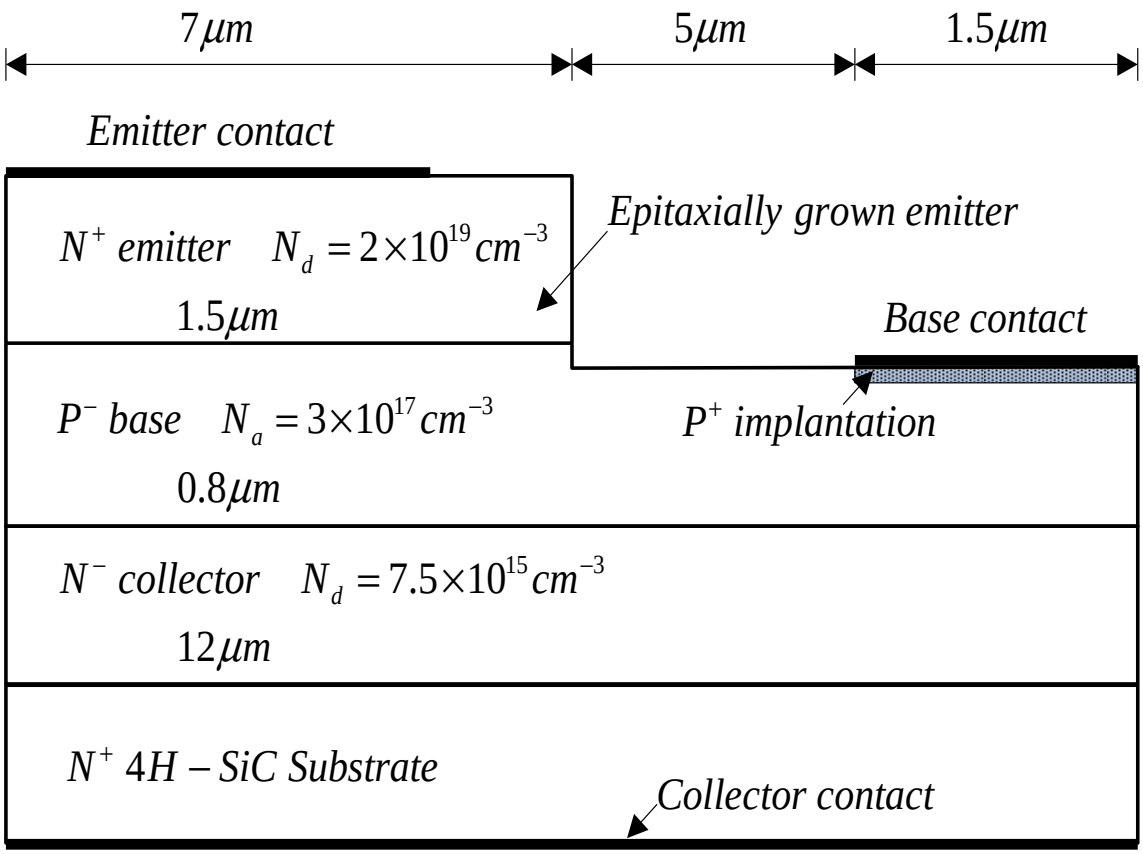

Figure 1. Schematic cross-section view of the 4H-SiC NPN BJT cell structure.

2.3 Drift Layer Design for Punch-Through Structure

For power device studied, a punch-through structure is used to support breakdown voltage. Figure1 shows the schematic cross sectional view of the 4H-SiC NPN BJT cell structure. This structure consists of three epilayers. The top N^+ layer is the emitter. The middle p-type epilayer is the base. The N^- layer (drift layer) between the N^+ collector and the P base is used to support the high breakdown voltage. The emitter mesa is etched into the P base layer by 0.2 *μm*. A thin, highly doped P^+ region can be formed by ion implantation under the base contact to reduce contact resistance. This structure is designed to be able to block near 2000 V under the optimum reach-through condition when the emitter is open. A 12 *μm*, $7\times10^{15}cm^{-3}$ doped n-type epilayer is chosen for the drift layer. The base doping concentration is $3.7\times10^{17}cm^{-3}$ and the base width is 0.8 *μm*. The emitter has a doping concentration of $2\times10^{19}cm^{-3}$ with a thickness of 1.5 *μm*.

The punch-through structure has a lower doping concentration on the lightly doped side with a high concentration contact region, and the thickness of the lightly doped side is smaller than that for non punch-through structure for equal breakdown voltages. In punch-through structure, the electric field varies less gradually with distance within the lightly

doped region, resulting in a rectangular electric field profile as compared to a triangular electric field profile for the non punch-through structure. The breakdown voltage for punch-through structure is given by [32]:

$$V_{BR} = E_{cr} W_P - \frac{qN^- W_p^2}{2\varepsilon_s} \quad (9)$$

where W_p and N^- are the thickness and doping concentration of the drift region (lightly doped region), respectively. Figure 2 shows the breakdown voltage calculated for the punch-through structure in 4H-SiC as a function of the drift region doping concentration. When the doping concentration and the thickness of the drift region become large, the breakdown voltage approaches that for the non punch-through structure. In addition, the breakdown voltage of the punch-through structure is a weak function of the drift region doping concentration if its thickness is small.

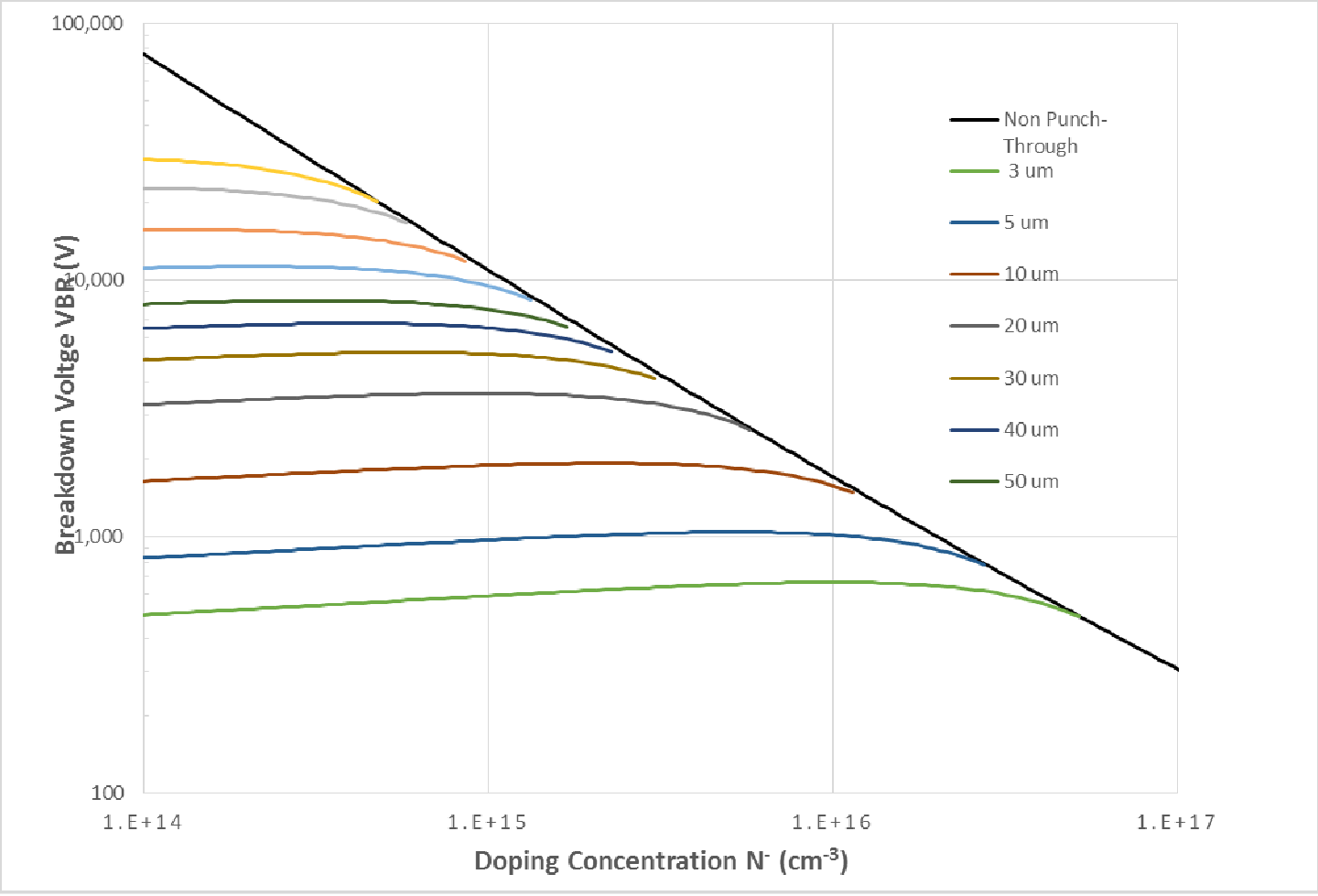

Figure 2. Dependence of the breakdown voltages in 4H-SiC punch-through structures on the drift region doping concentration.

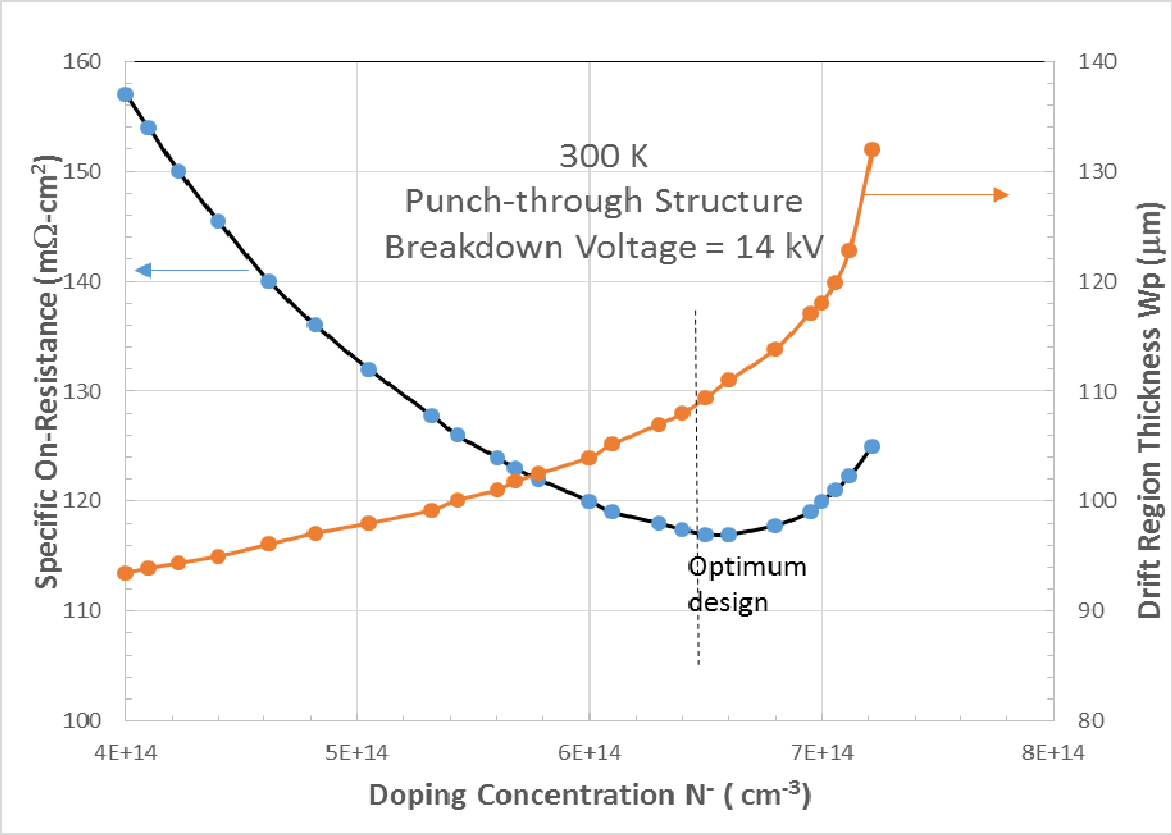

Figure 3. Optimization of the drift region doping concentration and thickness for a 14 kV punch-through structure in 4H-SiC at 300 K.

For a given breakdown voltage, the drift region thickness and doping concentration of punch-through structure can be optimized to give the lowest specific on-resistance. Figure 3 illustrates such an optimization scheme performed for a breakdown voltage of 14 kV at 300 K. The optimum drift region thickness and doping concentration are 114 *μm* and $6.6\times10^{14}cm^{-3}$, respectively, which gives the lowest specific on-resistance of 117 mΩcm^2. The optimum drift region thickness and doping concentration for 4H-SiC punch-through structure at different breakdown voltages are presented in Figure 4. The optimum specific on-resistance is compared with the theoretical specific on-resistance of non punch-through structure in Figure 5, where the optimized punch-through structure not only has a thinner drift region, but also has a slightly lower specific on-resistance than non punch-through structure.

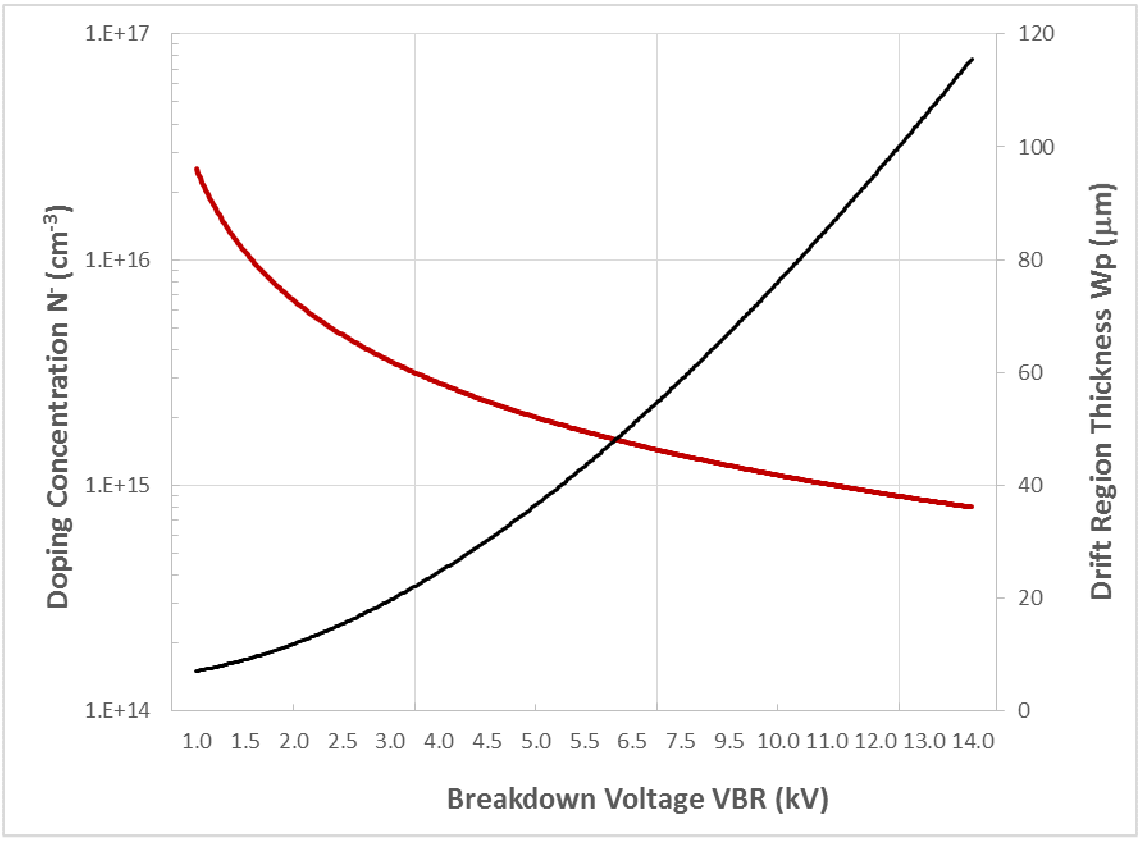

Figure 4. **Optimized doping concentration and thickness for the drift region of 4H-SiC punch-through structure.**

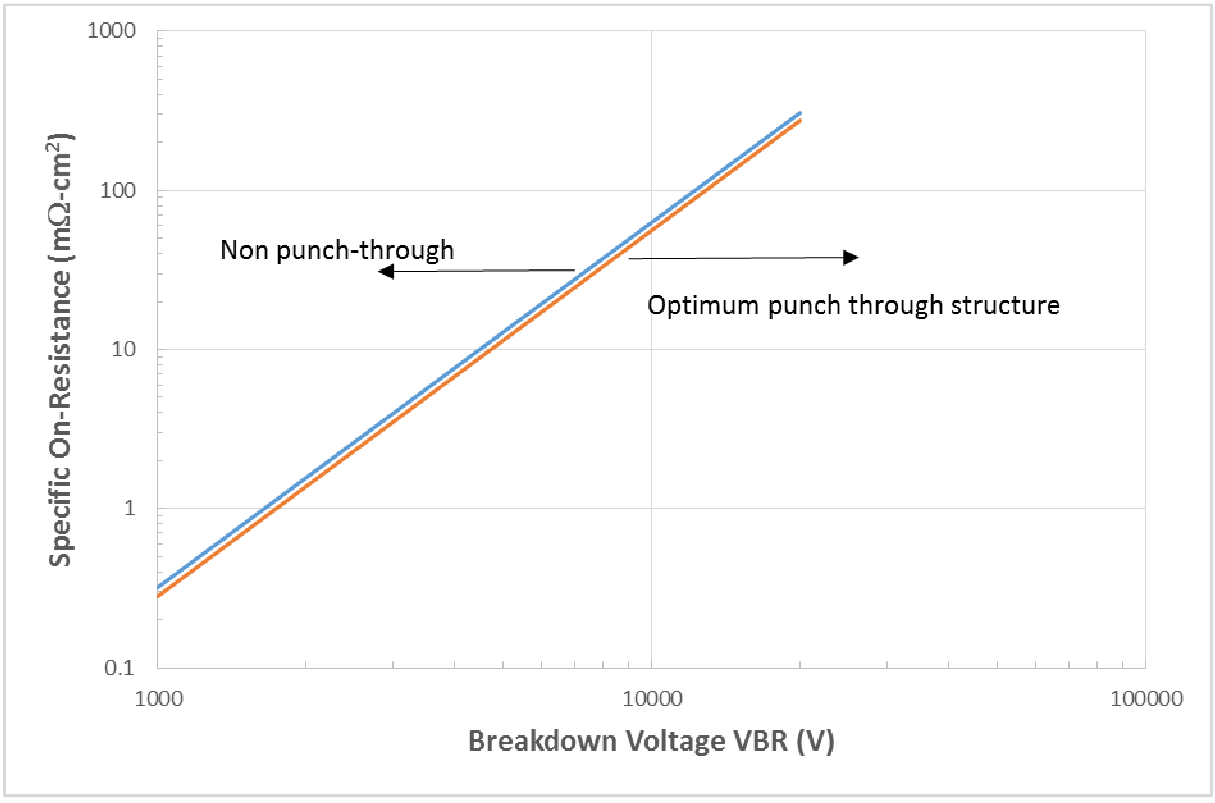

Figure 5. Comparison of the optimized specific on-resistance of 4H-SiC punch-through structure with that of non punch-through structure.

The simulated blocking characteristics of the 4H-SiC NPN BJT are shown in Figure 6 . The device is able to block 1941 V and 2094 V at 300 K and 523 K, respectively, when the emitter is open. When the base is open, the device can block 1631 V and 2033 V at 300 K and 523 K, respectively. The blocking voltage is smaller when the base is due to the current-amplifying properties of the common emitter connection.

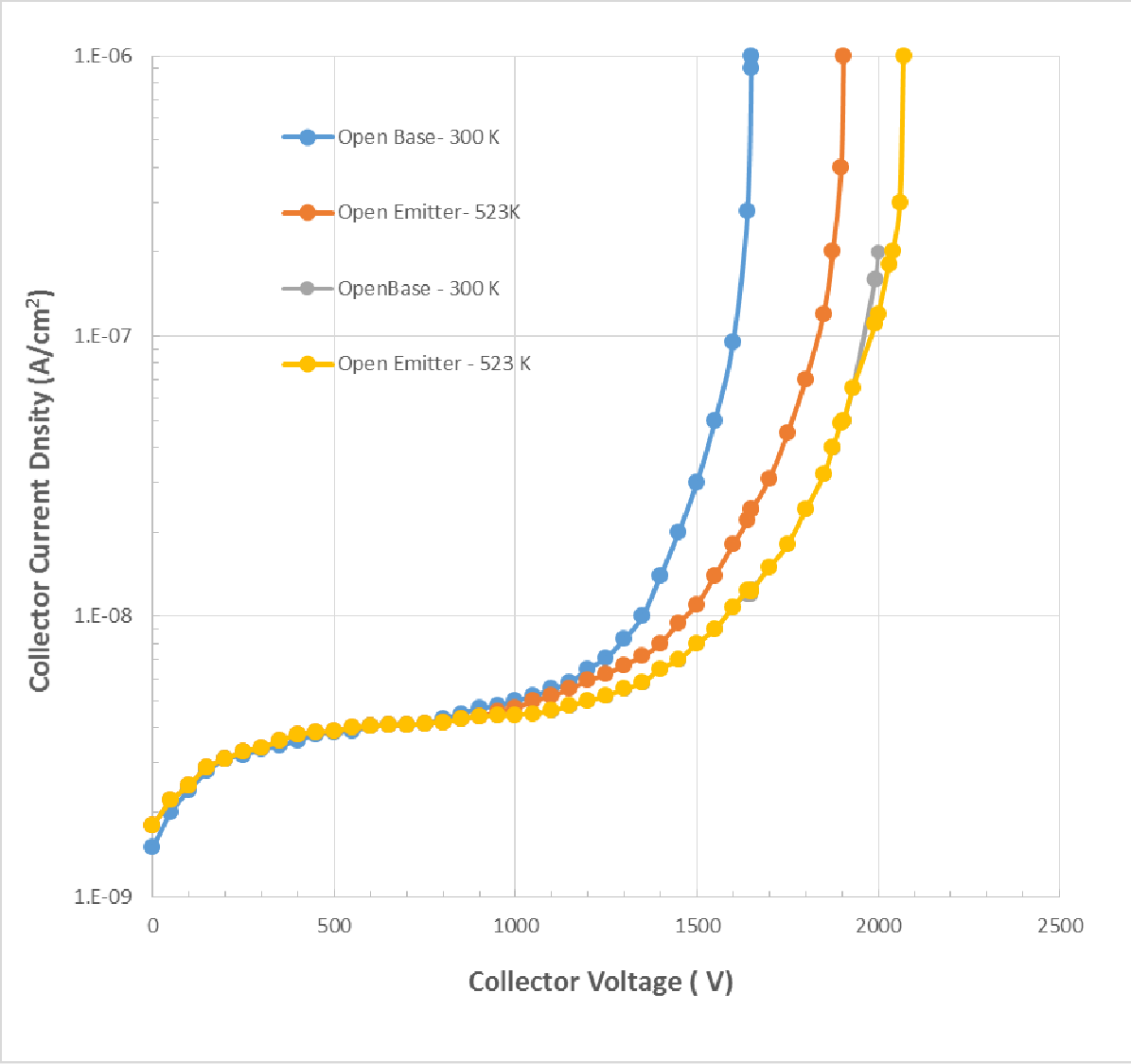

Figure 6. Simulated blocking characteristics of the 4H-SiC NPN BJT at 300 K and 523 K.

3. Comparison with Experimental Data and Discussions

For a power device with an n-type lightly doped drift layer, the blocking junction can be approximated with an one-side abrupt p^+n junction theory. In the blocking state the depletion region mainly extends into the lightly doped drift region and the maximum electric field in the depletion region is given by:

$$E_{\max} = \sqrt{\frac{2qN_D V_a}{\varepsilon_s}} \quad (10)$$

Where *Va* is the applied bias. From equation (10), it can be seen that the maximum electric field in the depletion region increases with increasing applied bias. For a non-punch through breakdown where impact ionization is the main cause of the breakdown, the ideal breakdown voltage V_{BR} for a given doping level N_D can be derived from Eq. (7) and Eq. (10) [32, 33]:

$$V_{BR} = \frac{\varepsilon_s E_{cr}^2}{2qN_D} \quad (11)$$

This equation shows that the non punch-through blocking voltage is about *143 V* much lower the blocking voltage reported in the experimental device. The experimental transistor shows a blocking voltage of about 1631 V at 300 K . The simulated blocking voltage is at 1600 V at 300 K which is in agreement with the experimental data [34]. As a result, the experimental structure presented in Figure 1 demonstrates a punch-through design discussed below. The punch through usually occurs when the doping concentration of the base layer becomes sufficiently low. At higher temperature the breakdown voltage increases as shown in Figure 6. One explanation is that hot carriers passing though the depletion region under high electric field lose part of their energy to optical phonons hence must travel through a greater potential difference and higher voltage before they can obtain sufficient energy to generate an electron-hole pair [35].

The structure of the experimental device is the same as the one shown in Figure 1 except that the emitter layer thickness is 0.7 *μm*. The device active area is 0.012 cm^2. The experimental data in this section is taken from [34]. The simulation parameters used in ATLAS program are given in Table 1. The measured and simulated I-V characteristics of the device at room temperature are shown in Figure 7. The experimental 4H-SiC BJT is able to block 1631 V at 300 K and to block 2033 V at 523 K, respectively and when base is open. The simulated blocking voltage when base is open is slightly lower (1600 V at 300 K) than the experimental value due to the current-amplifying properties of the common-emitter BJT.

The collector current (I_C) is measured up to 4.41 A (current density of J_C = 368 A/cm^2) at a base current (I_B) of 140 mA, corresponding to a common emitter current gain of 31 at collector emitter voltage of V_{CE} = 8 V. The maximum current gain is 32 at J_C =319 A/cm^2. The specific on-resistance is 17 mΩcm^2 measured at V_{CE} =5 V and I_B = 140 mA. The open-base blocking voltage is near 1600V at room temperature, where the leakage current is only 1.2 mA. The simulation parameters used in Figure 7 are summarized in Table 2. This result represents state of the art for 4H-SiC NPN BJTs with both high blocking capability and high current gain at high current density.

Table. 2 Simulation Parameters

Parameters	**Values**
Base region	
Electron Mobility	347 cm^2/Vs
Electron Lifetime	22 ns
Emitter region	
Hole Mobility	34.5 cm^2/Vs
Hole lifetime	5.7 ns
Collector series resistance, R_C	1.24 Ω

The theoretical specific on-resistance of the experimental BJT is about 1.5 $m\Omega cm^2$ (assuming the maximum electron mobility is 947 cm^2/Vs), which is about 11 times lower than the measured specific on-resistance. The high measured specific on-resistance may not be due to the low electron mobility because the device has a high current gain. The fitting to the measured *I-V* characteristics cannot be achieved by using low electron mobility even when the maximum carrier lifetimes are as high as 5 μs. At present, it is actually not well understood why the measured specific on-resistance is so high. Thus, a resistor of 1.24 Ω is connected to the collector in order to fit the specific on-resistance of the device.

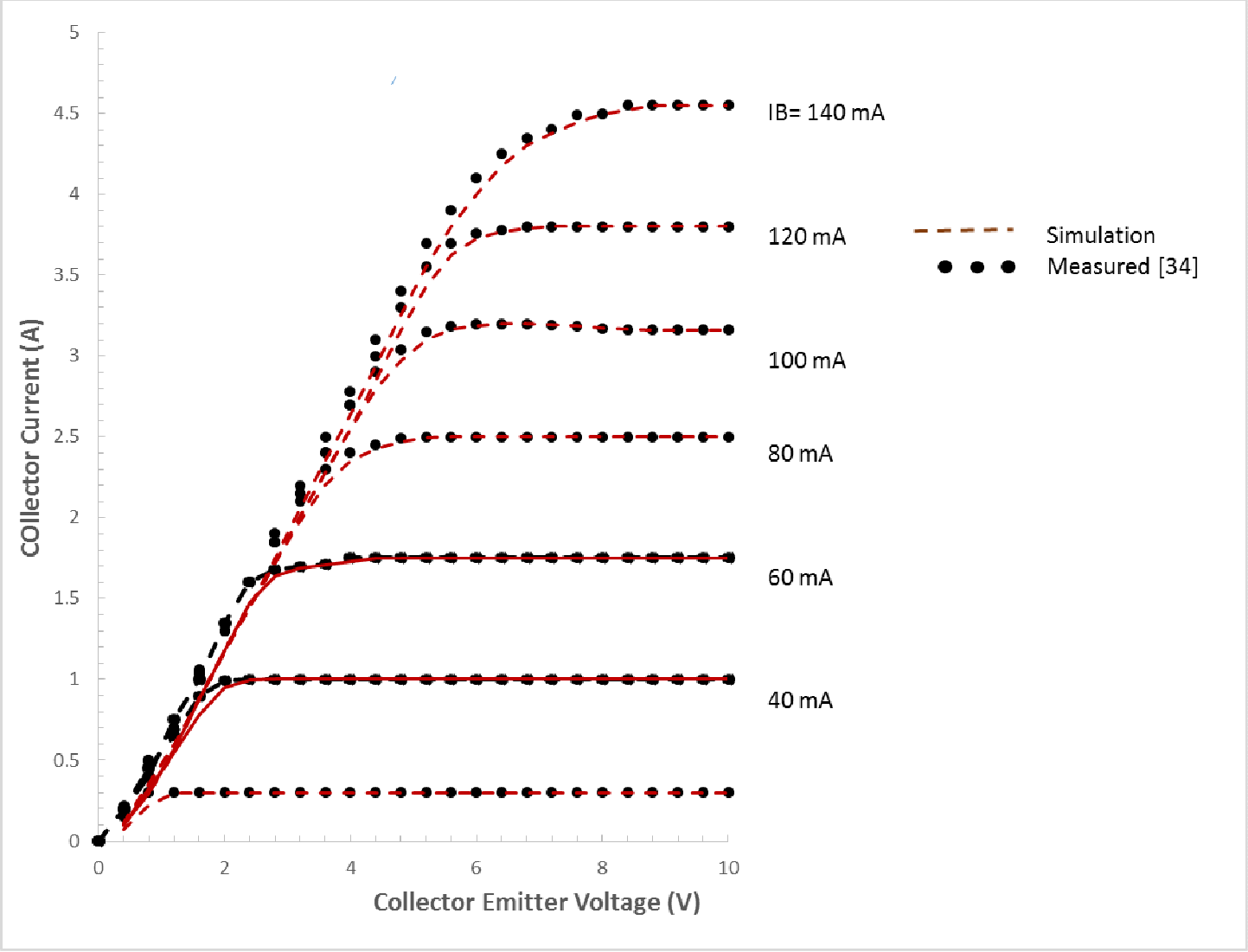

Figure 7. Measured and simulated output characteristics (I_C vs. V_{CE}) of the fabricated 4H-SiC NPN BJT at room temperature; the measured data is taken from [34].

4. Conclusion

The specific on-resistance is compared with the theoretical specific on-resistance of non punch-through structure. It is shown that the optimized punch-through structure not only has a thinner drift region, but also has a slightly lower specific on-resistance than non punch-through structure. The model is applied and compared to a measured 4H-SiC bipolar transistors with high blocking voltage and results are discussed. The experimental 4H-SiC BJT is able to block 1631 V at 300 K and 2033 V at 523 K, respectively when the base is open. The simulated blocking voltage when base is open is slightly lower (1600 V at 300 K) than the experimental value due to the current-amplifying properties of the common-emitter BJT.

References

[1] Miyake, H., Okuda, T., Niwa, H., Kimoto, T., and Jun Suda, J., 2012. 21-kV SiC BJTs With Space-Modulated Junction Termination Extension", IEEE Electron Device Letters, vol. 33, no. 11, pp. 1598-1600.

[2] Ryu, S.H., Capell, C., Jonas, C., Cheng, L., O'Loughlin, M., Burk, A., Agarwal, A., and Palmour, J., Hefner, A., 2012. Ultra High Voltage (>12 kV), High Performance 4H-SiC IGBTs, Proceedings of the 2012 24th International Symposium on Power Semiconductor Devices and ICs, 3-7 June 2012 - Bruges, Belgium.

[3] Zetterling, C. M, 2002. Process technology for silicon carbide devices, in EMIS processing series, IEE.

[4] Chow, T. P., 2000. SiC and GaN High-Voltage Power Switching Devices, Materials Science Forum, vol.338, p. 1155.

[5] Choyke, W. J. and Pensl, G. 1997. Physical Properties of SiC, in MRS Bulletin, vol. 22, p. 25.

[6] Bhalla, A. and Chow, T.P., 1994. Bipolar Power Device Performance: dependence on materials, lifetime, Proc. of the 6th Internat. Symposium on Power Semiconductor Devices & IC's, Davos, Switzerland, May 31 - June 2, 1994, pp. 287-291.

[7] Lee, H.-S., Domeij, M., Zetterling, C.-M., OÌˆstling, M., Allerstam, F., SveinbjoÌˆrnsson, E. OÌˆ, 2008. Surface passivation oxide effects on the current gain of 4H-SiC bipolar junction transistors, Applied Physics Letters, vol. 92, no.8, pp.082113, 2008, ISSN: 00036951.

[8] Zolper, J. E., 2005. Emerging silicon carbide power electronics components, IEEE Applied Power Electronics Conference and Exposition (APEC), pp.11-17.

[9] Xiao-Yan, T., Qing-Wen, S., Yu-Ming, Z., Yi-Men, Z., Ren-Xu, J., Hong-Liang, L., and Yue-Hu, W., 2012. Investigation of a 4H SiC metal insulation semiconductor structure with an Al2O3/SiO2 stacked dielectric, Chin. Phys. B., vol. 21, no. 8, 087701.

[10] Qian, Z., Yu-Ming, Z., Lei, Y., Yi-Men, Z., Xiao-Yan, T., and Qing-Wen, S., 2012. Fabrication and characterization of 4H SiC bipolar junction transistor with double base epilayer, Chin. Phys. B., vol. 21, no. 8, 088502.

[11] Silvaco International Software, 2005. Atlas User's Manual, Santa Clara, CA, USA. [12] Yong-Hui, D., Gang, X., Tao, W., and Kuang, S., 2013. A novel 4H-SiC lateral bipolar junction transistor structure with high voltage and high current gain, Chin. Phys. B vol. 22, no. 9,097201.

[13] Pâques, G., Scharnholz, S., Dheilly, N., Planson, D., and De Doncker, R., 2011. High-Voltage 4H-SiC Thyristors With a Graded Etched Junction Termination Extension, IEEE EDS, vol. 32, no.10.

[14] Bellotti, E., Nilsson, H.E., and Brennan, K.F. 2000. Monte Carlo calculation of hole initialed impact ionization in 4H phase SiC, J. Appl. Phys., vol.87, no.8, pp. 864-3871.

[15] Niwa, H., Feng G., Suda, J., and Kimoto, T., 2012. Breakdown characteristics of 12–20 kV-class 4H-SiC PiN diodes with improved junction termination structures, Proceedings of the 2012 24th International Symposium on Power Semiconductor Devices and ICs, 3-7 June 2012 - Bruges, Belgium, pp.381-384.

[16] Imhoff, E.A., Kub, F. J., Hobart, K. D., \ Ancona, M.G., VanMil, B.L., Gaskill, D. K., Keong K.L., Myers-Ward R. L., and Eddy, Jr. C. R., 2011. High-Performance Smoothly Tapered Junction Termination Extensions for High-Voltage 4H-SiC Devices, IEEE EDS, vol. 58, no.10.

[17] Feng, G., Suda, J., and Kimoto, T., 2012. Space-Modulated Junction Termination Extension for Ultrahigh-Voltage p-i-n Diodes in 4H-SiC, IEEE EDS, vol. 59, no.2.

[18] Prasad, R., 2013. Application of Low Specific on Resistance and High Thermal Stability 6H –SIC DIMOSFET using with Uniform Distribution in the Drift Region," International Journal of Scientific and Research Publications, vol. 3, Issue 6, June 2013 1 ISSN 2250-3153.

[19] Kimura, R., Uchida, K, Hiyoshi, T., Sakai, M., Wada, K., and Mikamura, Y., 2013. SiC High Blocking Voltage Transistor, SEI Technical Review, no. 77.

[20] Qing-Wen, S., Yu-Ming, Z., Ji-Sheng, H, Tanner, P., Dimitrijev, S., Yi-Men, Z., Xiao-Yan, T., and Hui, G., 2013. Fabrication and characterization of 4H SiC power UMOSFETs, Chin. Phys. B., vol. 22, no. 2, 027302.

[21] Hatakeyama, Y., Nomoto, K., Kaneda, N., Kawano, T., Mishima, T., and Nakamura, T., 2011. Over 3.0 GW/cm2 Figure-of-Merit GaN p-n Junction Diodes on Free-Standing GaN Substrates, IEEE ED Letter, vol. 32, no.12.

[22] Hatakeyama, Y., Nomoto, K., Terano, A., Kaneda, N., Tsuchiya, AT., Mishima, TY., and Nakamu, T., 2013. High-Breakdown-Voltage and Low-Specific-on-Resistance GaN p–n Junction Diodes on Free-Standing GaN Substrates Fabricated Through Low-Damage Field-Plate Process," Japanese Journal of Applied Physics, 52, 028007.

[23] Mochizuki, K., Mishima, T., Terano, A., Kaneda, N., Ishigaki, T., and Tsuchiya, T., 2011, Numerical Analysis of Forward-Current/Voltage Characteristics of Vertical GaN Schottky Barrier Diodes and p-n Diodes on Free-Standing GaN Substrates, IEEE EDS, vol. 58, no.7.

[24] Nomoto, K., Hatakeyama, Y., Katayose, H., Kaneda, N., Mishima, T., and Nakamura, T., 2011. Over 1.0 kV GaN p–n junction diodes on free-standing GaN substrates, Phys. Status Solidi A 208, no. 7, 1535–1537.

[25] Ryu, S. H., Agarwal, A. K., Singh R., and Palmour, J. W. 2001. 1800V NPN bipolar junction transistors in 4H-SiC, IEEE Electron Device Letters, vol. 22, p. 124.

[26] Zhang, J., Zhao, J.H., Alexandrov, P., and Burke, T., 2004. Demonstration of first 9.2kV 4H-SiC bipolar junction transistor, Electronics Letters, vol. 40, p. 1381.

[27] Zhang, J., Alexandrov, P., T. Burke, and Zhao, J. H., 2006. 4H-SiC power bipolar junction transistor with a very low specific on-resistance of 2.9 $m\Omega cm^2$, IEEE Electron Device Letters, vol. 27, p. 368.

[28] Chynoweth, G., 1958. Ionization rates for electrons and holes in Silicon, Physics Review, vol. 109, no.5, pp. 1537-40.

[29] Raghunatha, R., and Baliga, B.J., 1999. Temperature dependence of hole impact ionization coefficients in 4H and 6H-SiC, Solid-States Electronics, vol.43, pp.199-211.

[30] Yokuto, Y., and Crowell, C.R., 1975. Threshold energy effects on avalanche breakdown voltage in semiconductor junctions, Solid-States Electronics, vol. 18, pp.161-168.

[31] Konstantinov, A.O., Wahab, Q., Nordell, N., and Lindefelt, U., 1997. Ionization rates and critical fields in 4H silicon carbide, Appl. Phys. Lett., 71(1), 90-92.

[32] Baliga, B.J., 1987. Modern Power Devices, New York: Wiley, 1987.

[33] Niu, X., 2010. Design and Simulation of 4H Silicon Carbide Power Bipolar Junction Transistors, MSEE thesis, University of Colorado, Denver.

[34] Luo, Y., Zhang, J.H., Alexandrov, P., Fursin, L. , Zhao, J.H., and Burke, T. 2003. High voltage (>lkV) and high current gain (32) 4H-SiC power BJTs using AI-free ohmic contact to the base, IEEE Electron Devices Letters, vol.24, no.11, pp.695-697.

[35] Sze, S.M. 1981. Physics of semiconductor devices, Wiley, New York.